Acta Crystallographica Section D
Biological Crystallography
ISSN 0907-4449

Crystallization, X-ray diffraction and oligomeric characterization of arginine decarboxylase from *Yersinia pestis*, a key polyamine biosynthetic enzyme

Chandra N. Patel, Robert S. Adcock, Korie G. Sell and Marcos A. Oliveira*

Department of Pharmaceutical Sciences, Markey Cancer Center and Center for Structural Biology, University of Kentucky, USA

Correspondence e-mail: moliv2@email.uky.edu

Received 11 June 2004
Accepted 26 October 2004

Arginine decarboxylase (ADC) is a 70 kDa pyridoxal-5′-phosphate (PLP) dependent enzyme that controls an alternative step in the biosynthesis of polyamines in some bacteria and plants. Crystals of ADC were flash-cooled and diffracted to 3.0 Å resolution using a synchrotron-radiation source. Crystals of ADC are monoclinic, with four monomers in the asymmetric unit. Light-scattering data reveals that the enzyme forms dimers in solution. The rotation function suggests the presence of two dimers in the asymmetric unit. Heavy-atom searches have identified PCMBS as forming a mercury derivative.

1. Introduction

Extensive documentation has shown the importance of polyamines for growth in a wide range of organisms including humans, parasites and bacterial pathogens (Wallace *et al.*, 2003). Many bacteria have two key polyamine biosynthetic enzymes, ornithine decarboxylase (ODC; EC 4.1.1.17) and arginine decarboxylase (ADC; EC 4.1.1.19), both of which are PLP-dependent enzymes. These enzymes control two key rate-limiting steps in the biosynthesis of polyamines. Arginine decarboxylase (ADC) is a pyridoxal-5′-phosphate (PLP) dependent enzyme that is found in most bacteria and in plants, but there is some controversy whether there is a homologous ADC enzyme in humans (Coleman *et al.*, 2004; Zhu *et al.*, 2004). In *Yersinia pestis* and *Pseudomonas aeruginosa* (Nakada & Itoh, 2003) the product of ADC, agmatine, is converted to the polyamine putrescine in two steps involving the enzymes agmatine deiminase (EC 3.5.3.12) and *N*-carbamoylputrescine amidohydrolase (EC 3.5.1.53). Putrescine is then converted to the polyamines spermine and spermidine by the addition of an aminopropyl group donated by decarboxylated *S*-adenosylmethionine (SAM), which is produced by SAM decarboxylase (SAMDC) (Fig. 1).

ADC belongs to the fold III PLP-dependent decarboxylases (Grishin *et al.*, 1995), which include alanine racemase (ALR; Shaw *et al.*, 1997), mammalian ornithine decarboxylase (ODC; Kern *et al.*, 1999) and diaminopimelate decarboxylase (DapDC; Gokulan *et al.*, 2003). Structures of all three enzymes are available and sequence comparison reveals that ADC has a similar fold. However, ADC has two distinctive features that are evident in a sequence alignment (Balbo *et al.*, 2003) with other fold III PLP-dependent decarboxylases of known structure. The first unique feature of ADC is an insertion of ∼70 residues localized between the TIM-barrel and β-sandwich domains (Balbo *et al.*, 2003). The second distinctive feature of ADC is the requirement of magnesium for activity (Wu & Morris, 1973).

2. Experimental methods and results

2.1. Protein purification and crystallization

The *Y. pestis speA* gene coding for ADC was cloned from genomic DNA. The pET-28b (Novagen) bacterial expression vector containing the recombinant *speA* gene was transformed into BL21(DE3)pLysE (Invitrogen) competent *Escherichia coli* cells. The expression vector was selected because of the incorporation of a C-terminal histidine tag as opposed to the standard N-terminal histidine tag. This is important because the purification of ADC reveals that the protein exists in two forms as observed in SDS–PAGE and IEF (data not shown). The existence of the two forms was originally observed in *E. coli* (Buch & Boyle, 1985; Moore & Boyle, 1990) and occurs because of the presence of an N-terminal signal sequence that targets ADC to the periplasm. We also cloned *speA* into pET-38b (Novagen) because this expression vector has a cleavable C-terminal histidine tag that can be removed by thrombin. The protein was purified as described by Balbo *et al.* (2003).

We used Hampton Crystal Screens I and II and the hanging-drop method with Limbro plates and protein concentrated in the range 10–20 mg ml^{-1}. The protein was prepared in cacodylate buffer pH 6.0. The buffer was chosen based on the pI (4.9) of ADC. The crystallization condition that gave optimal

crystals was a combination of PEG 8000 and 2-propanol [condition No. 41 from Hampton Crystal Screen I; 10%(*w*/*v*) 2-propanol, 20%(*w*/*v*) PEG 4000, 0.1 *M* HEPES pH 7.5]. The first crystals produced were small thin plates (less than 0.1 mm in their largest dimension). All diffraction characterization of ADC was performed at the Advanced Photon Source (APS) at Argonne, IL, USA, since only low-resolution (less than 7 Å) diffraction was observed at our home source (R-AXIS IV). Optimal flash-cooling conditions were achieved by exchanging 2-propanol for ethylene glycol during the crystallization setup. Flash-cooling conditions also generated larger and more reproducible crystals (~0.2–0.3 mm) (Fig. 2).

2.2. Dynamic light-scattering and oligomeric state

Experiments were performed with both holo-ADC (92.5 µ*M*) with bound cofactors (PLP and Mg^{+}) and the apo form of ADC (95.6 µ*M*). The holo-ADC solution had a mean polydispersity of 1.0 nm and a monomodal fit of the data indicated a molecular weight of 178 kDa, which is consistent with a dimer in solution at pH 8.0. The polydispersity index suggested conditions suitable for crystallization. The apo-ADC had a polydispersity of 1.2 nm and a monomodal fit gave a molecular weight of 163.1 kDa. Briefly, dynamic light-scattering measurements were performed using a DynaPRO99 instrument (Protein Solutions). ADC was concentrated to approximately 10 mg ml^{-1} in 0.1 *M* HEPES pH 8.0, 10 m*M* MgCl, 50 µ*M* PLP. The protein solution was filtered through 0.1 µm Anodisc 13 membrane filters (Whatman) to remove any residual gas bubbles or solid impurities. *Dynamics* v.5.25.44 software was used in the data collection and analysis. The number of acquisition scans was 44 for holo-ADC and 27 for apo-ADC and the acquisition time was 3 s per scan at 295 K. The oligomeric states of the both holo-enzyme and the apo-enzyme based on dynamic light scattering suggest that ADC is a dimer at pH 8.0 regardless of the presence or absence of PLP and magnesium.

2.3. X-ray diffraction

We collected several native data sets from ADC at beamline 22-ID at APS Argonne, IL, USA (λ = 1 Å). Data sets were processed to 3.0 Å using *HKL*2000 (Table 1). Given the unit-cell parameters of the ADC crystals (Table 1) and the molecular weight of the dimer, crystals of ADC can be estimated to contain four monomers in the asymmetric unit. A calculation of a self-rotation function using the program *GLRF* (Tong & Rossmann, 1997) allows identification of the molecular twofold axis. A stereographic projection of the rotation function for $\kappa = 180$ (twofold peaks) is shown in Fig. 3. The largest peak ($\varphi = 90$, $\psi = 0^{\circ}$) corresponds to the crystallographic twofold axis of the space-group symmetry $P2_1$. The other non-

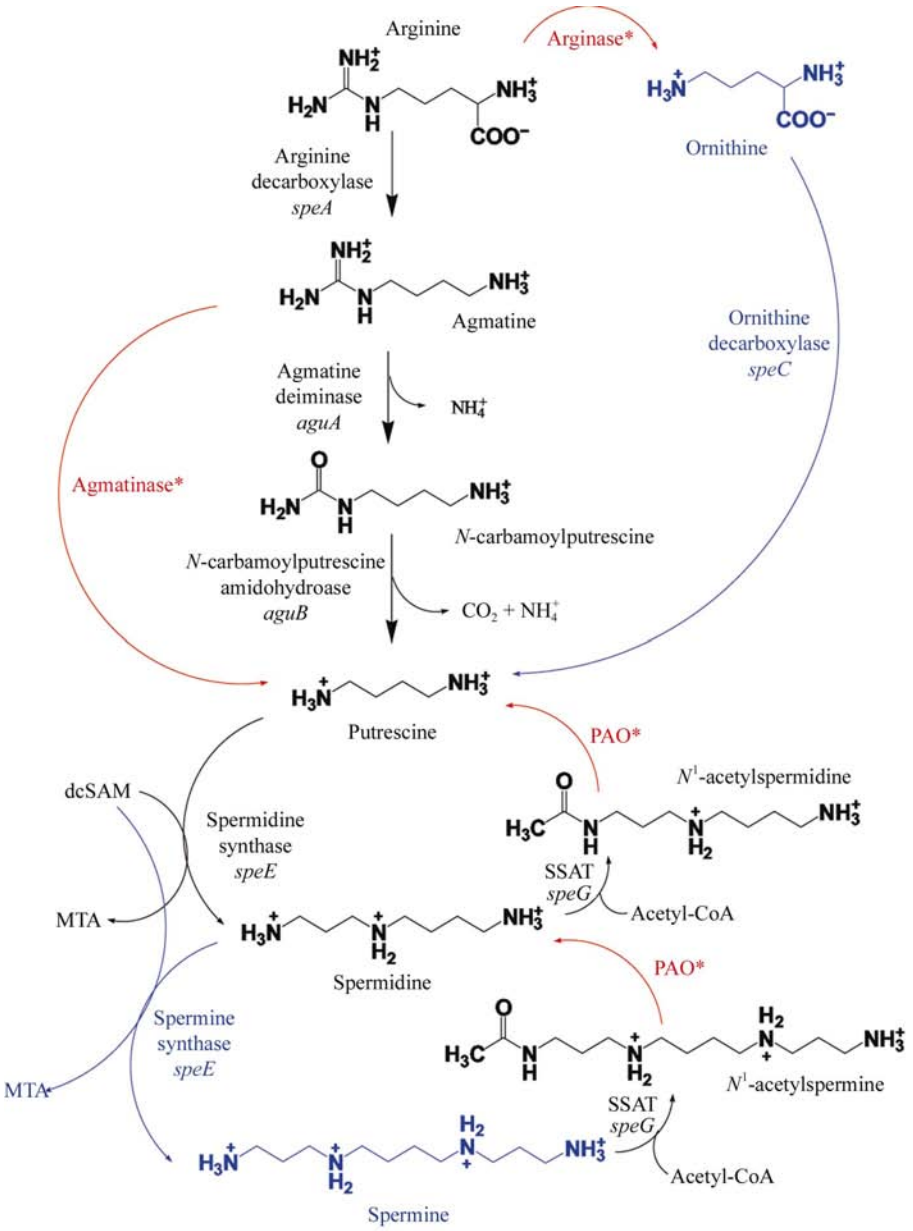

Figure 1
A general polyamine pathway. Asterisks indicate steps not found in some other bacteria.

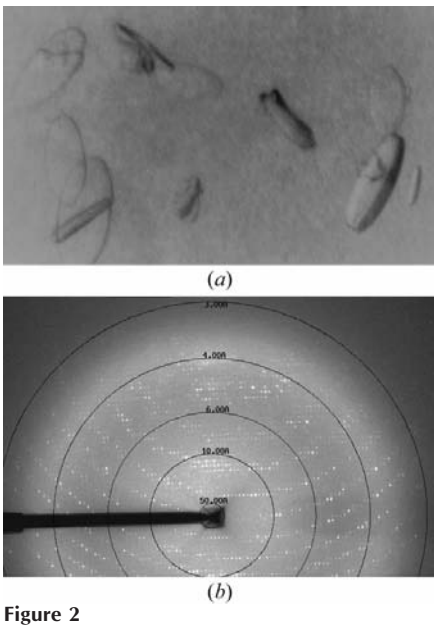

Figure 2
(*a*) Crystals of ADC are oval; the largest dimension is 0.3 mm. (*b*) A representative diffraction pattern collected at the SERCAT-ID22 beamline at APS, Argonne, IL, USA.

Table 1
Crystallographic parameters of ADC crystals and data-collection statistics.

Unit-cell parameters (Å)	
a	116.5
b	78.0
c	147.3
V (Å^3)	1343663
Space group	$P2_1$
Dimer MW (kDa)	74
Dimers in AU	2
V_M (Å^3 Da^{-1})	2.4
Redundancy	5
Resolution (Å)	3.0
Wavelength (Å)	1.0
No. crystals	1
Exposure time (s)	3
Beamline	22-ID, APS
R_{merge} (%)	14.5
Completeness (%)	94
$I/\sigma(I)$	5

crystallographic peaks are consistent with two dimers in the asymmetric unit.

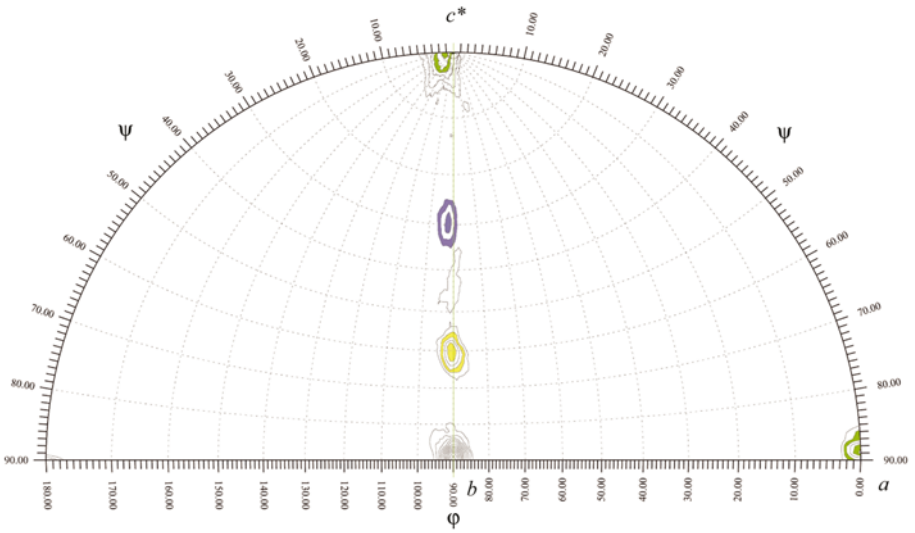

Figure 3
Rotation function, $\kappa = 180$. There are five peaks ($\varphi = 90$, $\psi = 0°$ is the crystallographic twofold axis). The data is consistent with the presence of two dimers in the AU.

2.4. Heavy-atom searches

We have also performed a heavy-atom search focusing on mercury compounds. The choice of mercury compounds was based on the observation that in solution we estimate that one cysteine site per monomer is modified by mercury compounds using the procedure described by Riddles *et al.* (1983). The mercury heavy-atom derivative of ADC was produced by adding 1 µl of a 5 m*M* solution of either PCMBS or EMTS to hanging drops for a period of 1–24 h. The drop was then diluted with stabilizing solution (40% ethylene glycol, 20% PEG 8000) and flash-cooled in liquid N_2. The derivative crystals showed an overall mosaic spread of 0.5° compared with native ADC (2.5°). A Patterson map of the PCMBS derivative revealed several peaks and the highest was selected. The heavy-atom position was refined in *MLPHARE* (from the *CCP*4 suite of programs; Collaborative Computational Project, Number 4, 1994; Winn, 2003). Difference Fourier maps were used to identify four heavy-atom positions that were refined with a final figure of merit of 0.3. There was some degree of non-isomorphism. Flash-cooled crystals displayed radiation decay. These two observations have required us to focus on collecting the best possible single anomalous dispersion data set. The strategy we have decided to use involves reducing the exposure time per oscillation and orienting crystals in order to maximize the detection of Friedel pairs in the same exposure.

We thank the American Association for Colleges of Pharmacy, who provided the initial support for this project through a New Investigator Award (NIP). We also thank the Kentucky Lung Cancer Research Program for partial support of this research. We thank Drs Robert Perry and Jacqueline Fetherston, who have been collaborating with us on the investigation of polyamine metabolism in *Y. pestis*. We thank Dr David Rodgers and his group for help and discussions. Data were collected at Southeast Regional Collaborative Access Team (SER-CAT) 22-ID (or 22-BM) beamline at the Advanced Photon Source, Argonne National Laboratory. Supporting institutions may be found at http://www.ser-cat.org/members.html. Use of the Advanced Photon Source was supported by the US Department of Energy, Office of Science, Office of Basic Energy Sciences under Contract No. W-31-109-Eng-38.

References

Balbo, P. B., Patel, C. N., Sell, K. G., Adcock, R. S., Neelakantan, S., Crooks, P. A. & Oliveira, M. A. (2003). *Biochemistry*, **42**, 15189–15196.
Buch, J. K. & Boyle, S. M. (1985). *J. Bacteriol.* **163**, 522–527.
Coleman, C. S., Hu, G. & Pegg, A. E. (2004). *Biochem. J.* **379**, 849–855.
Collaborative Computational Project, Number 4 (1994). *Acta Cryst.* D**50**, 760–763.
Gokulan, K., Rupp, B., Pavelka, M. S. Jr, Jacobs, W. R. Jr & Sacchettini, J. C. (2003). *J. Biol. Chem.* **278**, 18588–18596.
Grishin, N. V., Phillips, M. A. & Goldsmith, E. J. (1995). *Protein Sci.* **4**, 1291–1304.
Kern, A. D., Oliveira, M. A., Coffino, P. & Hackert, M. L. (1999). *Structure Fold. Des.* **7**, 567–581.
Moore, R. C. & Boyle, S. M. (1990). *J. Bacteriol.* **172**, 4631–4640.
Nakada, Y. & Itoh, Y. (2003). *Microbiology*, **149**, 707–714.
Riddles, P. W., Blakeley, R. L. & Zerner, B. (1983). *Methods Enzymol.* **91**, 49–60.
Shaw, J. P., Petsko, G. A. & Ringe, D. (1997). *Biochemistry*, **36**, 1329–1342.
Tong, L. & Rossmann, M. G. (1997). *Methods Enzymol.* **276**, 594–611.
Wallace, H. M., Fraser, A. V. & Hughes, A. (2003). *Biochem. J.* **376**, 1–14.
Winn, M. D. (2003). *J. Synchrotron Rad.* **10**, 23–25.
Wu, W. H. & Morris, D. R. (1973). *J. Biol. Chem.* **248**, 1696–1699.
Zhu, M. Y., Iyo, A., Piletz, J. E. & Regunathan, S. (2004). *Biochim. Biophys. Acta*, **1670**, 156–164.